SF2A 2011
G. Alecian, K. Belkacem, R. Samadi and D. Valls-Gabaud (eds)

SEARCH FOR LORENTZ INVARIANCE VIOLATION WITH AGNS: A PROSPECT FOR CTA

J. Bolmont[1] and A. Jacholkowska[1]

Abstract. In the recent years, many results have been published about a possible violation of Lorentz Invariance in the frame of Quantum Gravity (QG) models measuring time delays in the arrival times of very high energy (VHE, >100 GeV) gamma-ray photons from distant flaring active galaxies. These photons have been detected by the current ground-based VHE Cherenkov detectors (HESS, MAGIC, VERITAS) and so far, no deviations in the speed of light in vacuum have been seen either for linear or for quadratic scales. The new generation of ground-based instruments "the Cherenkov Telescope Array" (CTA) will be able to probe deeper into this area due to its increased sensitivity (one order of magnitude better than the current detectors) and broader energy range (above 10 GeV). Based on a maximum likelihood technique, a quantitative study is presented of the potential of CTA to detect possible QG effects. In addition, different array configurations are compared in an attempt to maximize the sensitivity to Lorentz Invariance Violation (LIV) effects.

Keywords: CTA, active galaxies, quantum gravity, Lorentz invariance violation

1 Quantum Gravity and Lorentz Invariance Violation

The search for a quantum theory of gravitation is one of the outstanding tasks of modern physics (Amelino-Camelia 2008). As an important consequence of the time-space discretization, Lorentz Invariance Violation (LIV) may appear as predicted in some models of Loop Quantum Gravity (Alfaro et al. 2002; Gambini & Pullin 1999) or String Theory (Ellis et al. 1999). The tiny effects in the photon propagation from distant astrophysical sources as Active Galactic Nuclei (AGNs) or Gamma-ray Bursts (GRBs) would add-up producing deviations in the value of the velocity of light (Amelino-Camelia 1998). These deviations could be represented by linear and quadratic terms in the so-called dispersion relation:

$$c^2p^2 = E^2\left(1 \pm \xi(E/M) \pm \zeta(E/M)^2 \pm ...\right), \tag{1.1}$$

where M is the Quantum Gravity energy scale (in principle close to the Planck scale) and ξ and ζ are positive parameters.

In this paper a search for LIV with photons emitted in flares of AGN is being presented as a prospect for the future Cherenkov Telescope Array (CTA) (CTA Consortium 2010). In section 2, the performance of the different possible array configurations, currently under evaluation with Monte Carlo simulations, are compared with the aim of maximizing the sensitivity to LIV effects. Then in section 3, the effect of potentially improved statistical accuracy due to both increased sensitivity and better energy coverage is evaluated.

2 Comparison of array configurations

The energy lever-arm ΔE is determined in order to compare the different array configurations, following to the spectrum simulation of a power law with EBL absorption (Mazin 2008) (for a redshift $z = 0.03$) and a break at 100 GeV representing the maximum of the Inverse Compton peak. The spectrum is then convoluted with the effective areas of different array configurations. Finally, the mean energy for low ($E < E_{lim}$) and high

[1] LPNHE, Université Pierre et Marie Curie Paris 6, Université Denis Diderot Paris 7, CNRS/IN2P3, 4 Place Jussieu, F-75252, Paris Cedex 5, France

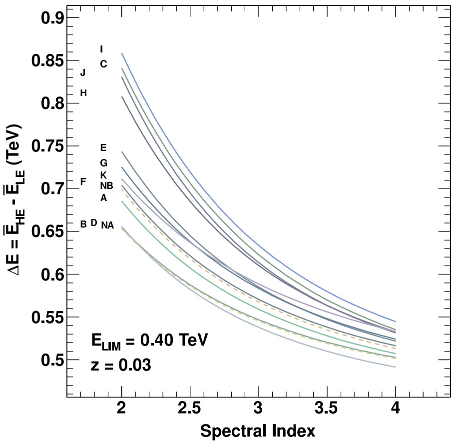

Fig. 1. Parameter ΔE as a function of the spectral index for all arrays considered in CTA Monte Carlo simulations. The configurations A to K are studied for Southern array and configurations NA and NB for the Northern array. The configurations have different layouts and number of telescopes CTA Consortium (2010).

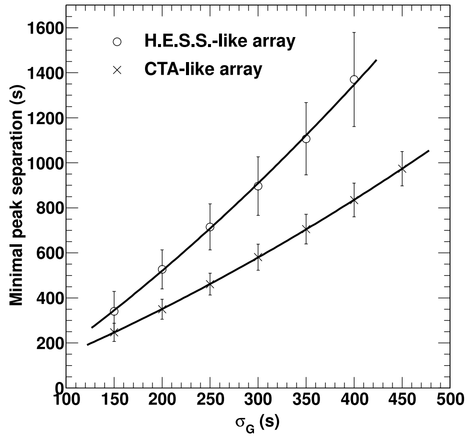

Fig. 2. Minimal distinguishable separation of the two peaks as a function of their width, in case of a H.E.S.S.-like (open circles) and a CTA-like measurement (crosses).

$(E > E_{lim})$ energy bands are computed and the difference $\Delta E = \bar{E}_{\rm HE} - \bar{E}_{\rm LE}$ is deduced. This way of comparing the different array configurations does not depend on the method used to compute the time lags.

Fig. 1 shows the parameter ΔE as a function of the spectral index for all arrays considered in CTA Monte Carlo simulations. E_{lim} is chosen to be optimal while preserving the highest statistics at high energies. This value is almost stable regardless of the array or spectral index used and lies around 500 GeV. Arrays which maximize ΔE are J, C, H, I for the Southern site and NB for the Northern array. The same ranking is obtained for the quadratic difference ΔE^2.

3 Effect of increased statistics

3.1 The analysis procedure

Here a likelihood fit procedure, as described in detail by Abramowski et al. (2011) and Martinez & Errando (2009), is used to measure the energy dependent time lags. This method makes use of individual photon information (energy and detection time) and requires a parameterization of both the light curve and the spectrum. The light curve is parameterized (function F_S) at low energies where the time lags are supposed to be negligible and the measured spectrum (Λ) is parameterized in the full energy range of the instrument. Then the probability density function (pdf) is given by:

$$P(t,E) = \int_0^\infty A(E_S)\Lambda(E_S)G(E-E_S,\sigma(E_S)) \, F_S(t-\tau_l E_S)dE_S, \tag{3.1}$$

where A is the acceptance of the detector and G takes into account the energy resolution of the detector, considered here to be 10%. After normalizing the pdf, the parameter τ_l (here for the linear correction to the dispersion relation of Eq. 1.1) is obtained by minimizing $-\ln(L)$ where

$$L = \prod_{\rm all\ photons} P(t,E). \tag{3.2}$$

A toy Monte Carlo software developed for PKS 2155-304 analysis (Abramowski et al. 2011) is used to simulate various sets of photons with given time and energy distributions. The injected lags range from -60 s $\rm TeV^{-1}$ to 60 s $\rm TeV^{-1}$ in steps of 20 s $\rm TeV^{-1}$ for the linear case and from -60 s $\rm TeV^{-2}$ to 60 s $\rm TeV^{-2}$ in steps of 20 s $\rm TeV^{-2}$

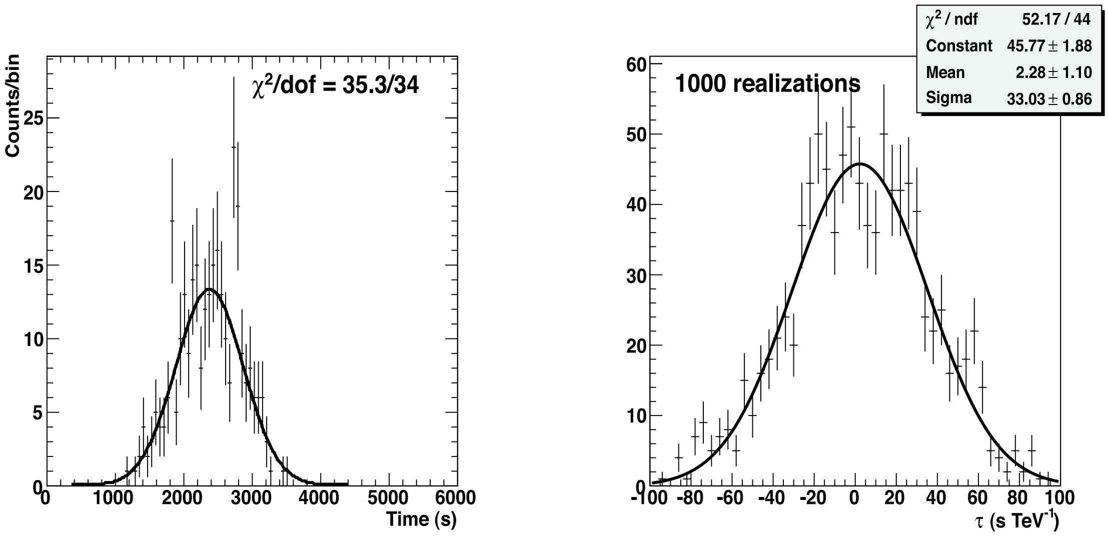

Fig. 3. Left: realization of a light curve with 300 photons and a binning of 60 s (H.E.S.S. case). The fit with a Gaussian curve leads to $\chi^2/\text{dof} = 35.3/34$. **Right**: distribution of the minimum of the likelihood for 1000 realizations of the lightcurve. The distribution if fitted with a Gaussian curve.

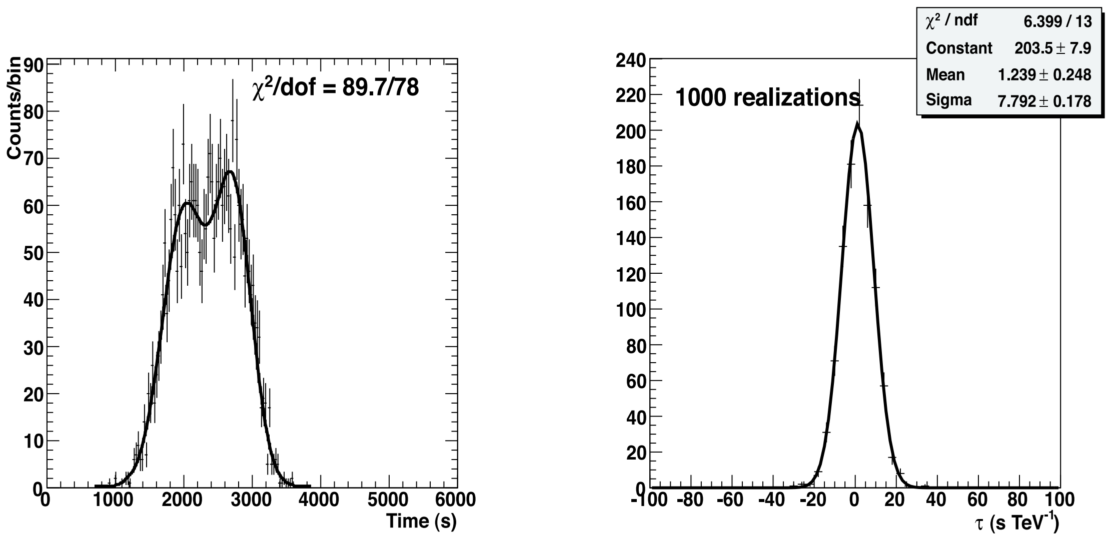

Fig. 4. Left: the flare of Fig. 3 (left) with 3000 photons and a binning of 30 s (CTA case). The fit with a double Gaussian curve leads to $\chi^2/\text{dof} = 89.7/78$. **Right**: distribution of the minimum of the likelihood for 1000 realizations of the lightcurve. The distribution is fitted with a Gaussian curve.

for the quadratic case. For each injected lag, 1000 realizations of the lightcurve are simulated. The obtained distribution of reconstructed lags is a Gaussian with standard deviation σ_τ. The mean dispersion $\bar{\sigma_\tau}$ is found as a standard deviation when fitting the distribution of Fig. 4 (right) and represents the calibrated error value used in further computation of the limits on LIV.

3.2 Peak separation capabilities

The likelihood fit procedure requires the measured light curve to be parameterized at low energies. As the error σ_τ is smaller when the spikes of the light curve are narrower, the peak separation capability is essential: a single peak seen by present day experiments could be observed with sub-structures with an instrument as CTA, which would in turn increase the performance of the analysis. In this section, this issue is studied using simple hypotheses.

A list of 3000 photons is generated randomly with energies following a power law distribution with index $\Gamma = 2.8$ and a time distribution chosen to be the sum of two Gaussian functions, which have the same standard deviation σ_G and the separation between the peaks is varied from 0 to 1400 s. The time distribution is fitted with one or two Gaussian functions. The bin width of the light curve is set to 60 s for H.E.S.S./MAGIC and to 30 s for CTA. The minimal peak separation is then obtained when $\chi^2/\mathrm{dof} = 1.5$.

Fig. 2 (previous page) shows the minimal peak separation necessary to distinguish the two spikes as a function of σ_G. For example, for two spikes of width $\sigma_G = 300$ s, a separation of at least 900 s is needed for H.E.S.S./MAGIC and only 500 s for CTA.

In order to quantify the effect of this result on the limits on $\mathrm{M_{LIV}}$, the likelihood was computed for $\sigma_G = 300$ s and a peak separation of 700 s.

As an example of this type of studies, Fig. 3 shows the fit of a realization of the light curve (left) and the distribution of likelihood minima for 1000 realizations (right) for an injected lag of 0 $\mathrm{s\,TeV^{-1}}$ and for 300 photons. The fit of the lightcurve with a single Gaussian curve gives a good value of $\chi^2/\mathrm{dof} = 35.3/34$.

Fig. 4 shows the same plots for 3000 photons. The two peaks are clearly visible and the light curve is fitted with the sum of two Gaussian functions. The lag reconstruction precision is improved by a factor of 5.

3.3 Lag reconstruction precision

In this section, the simulated time distribution of photons is considered to be a Gaussian curve with a standard deviation of σ_P. The energy distribution follows a power law $E^{-\Gamma}$ with index $\Gamma = 3.4$ (corresponding to PKS 2155-304 data recorded by H.E.S.S. in 2006 flare Aharonian et al. (2007)).

As expected, the average error $\bar{\sigma_\tau}$ on the reconstructed lag as a function of the number N_L of photons included in the likelihood fit computation (*ie* photons in the energy range of 0.3–10 TeV) follows the relation:

$$\bar{\sigma_\tau} \sim 1/\sqrt{N}. \tag{3.3}$$

In addition, and as already pointed out by Abramowski et al. (2011), when the width of the light curve peak σ_P increases, $\bar{\sigma_\tau}$ increases as well. This is related to the fact that the error on the lag is strongly dependent on the variability amplitude of the source.

As a conclusion at this step, it is expected that a flare like the one of PKS 2155-304 in July 2006 would lead to an error of <1 $\mathrm{s\,TeV^{-1}}$ (considering systematic and statistical effects) with CTA.

4 Discussion

The simulations performed for this work show that CTA will greatly improve the sensitivity of photon propagation studies with respect to LIV effects. Considering the fact that the sensitivity will be ten times higher than the one of present-day experiments and that the energy range covered will be much larger, the Planck scale will be easily reached for the “linear” models, comforting the present *Fermi* and H.E.S.S. results (Abdo et al. 2009a,b; Abramowski et al. 2011). In case of a flare as the one of Mkn 501 seen by MAGIC, Planck scale will be reached for the linear correction to the dispersion relations while a flare as the one seen by H.E.S.S. with PKS 2155-304 would largely exceed this value. The main increase in sensitivity will be reflected in the LIV scale in case of the “quadratic” models where a new range of detection will emerge. In particular, taking into account the best array configurations of section 2, the limits for the quadratic term of the dispersion relation should be higher than 10^{12} GeV.

Another important question for future studies is how many AGN flares will be observed by CTA. Of all flares observed so far, only three had enough statistics and high variability to be used for search of LIV. It is expected that CTA will detect tens of AGN flares per year, especially in the so-called “survey pointing mode” where each telescope points at different locations of the sky, allowing a higher probability to detect transient events. This will allow to increase the sensitivity to LIV effects by use of stacking procedures.

We gratefully acknowledge the support of GdR PCHE in France.

References

Abdo, A. A., Ackermann, M., Arimoto, M. et al. (Fermi LAT Collaboration) 2009, Science Express, 02/19/2009

Abdo, A. A., Ackermann, M., Arimoto, M. et al. (Fermi LAT Collaboration) 2009, Nature, 462, 331
Abramowski, A., Acero, F., Aharonian, F. et al. (H.E.S.S. Collaboration) 2011, Astropart. Phys., 34, 738
Aharonian, F., Akhperjanian, A. G., Bazer-Bachi, A. R., et al. (H.E.S.S. Collaboration) 2007, ApJL, 664, L71
Albert, J., Aliu, E., Anderhub, H. et al. (MAGIC Collaboration) 2007, ApJ, 669, 862
Albert, J., Aliu, E., Anderhub, H. et al. (MAGIC Collaboration) 2008, Phys. Lett. B, 668, 253
Alfaro, J., Morale-Técotl, H. A. & Urrutia, L. F. 2002, Phys. Rev. D, 65, 103509
Amelino-Camelia, G., Ellis, J., Mavromatos, N. E. et al. 1998, Nature, 395, 525
Amelino-Camelia, G. 2008, arXiv:0806.0339
CTA Consortium 2010, arXiv:1008.3703, `http://www.cta-observatory.org`
Ellis, J., Mavromatos, N. E. & Nanopoulos, D. V. 1999, Phys. Rev. D, 61, 027503
Gambini, R. & Pullin, J. 1999, Phys. Rev. D, 59, 124021
Martinez, M. & Errando, M. 2009, Astropart. Phys., 31, 226
Mazin, D. 2008, in Science with the New Generation of High Energy Gamma-Ray Experiments, eds. Scineghe